Joint EUROMECH / ERCOFTAC Colloquium 549
"Immersed Boundary Methods: Current Status and Future Research Directions"
Leiden, The Netherlands, 17-19 June 2013

Influence of caudal fin rigidity on swimmer propulsion efficiency

M. Bergmann[1], A. Iollo[1] and R. Mittal[2]

[1] Inria, F-33400 Talence, France. Univ. Bordeaux, IMB, UMR 5251, F-33400 Talence, France. CNRS, IMB, UMR 5251, F-33400 Talence, France. michel.bergmann@inria.fr

[2] Department of Mechanical Engineering, Johns Hopkins University, Baltimore, Maryland 21218, USA.

ABSTRACT

Quantitative evaluation of the mechanical characteristics of swimming is experimentally challenging. Reproducing the experimental setting is hard due to the complexity and variability of the geometries involved. Even harder is the accurate characterization of swimming laws and precise measurement of forces and power. For robotic propulsion, an experimental study in this direction is that of [1]. Ideally, numerical simulation can contour some of these difficulties. However, only a few numerical investigations of three-dimensional swimming modes have been attempted so far [5]. Here, we use numerical simulation to study a specific aspect of fish-like swimming: the influence of caudal fin deformation on performance. Previous numerical [3] and experimental [4] studies were dedicated to the effect of pectoral fin deformation on the local flow patterns. In particular, [4] found that there exist optimal fin flexural rigidity for maximizing thrust. We evaluate performance thanks to a non-dimensional index taking into account the total mechanical power acting on the fluid, the swimmer velocity and the force exerted in the locomotion direction [6]. In this paper we quantitatively investigate the efficiency improvement obtained by a simple and local modification of the caudal swimmer deformation. We concentrate on locomotion at low Reynolds numbers, so that all the relevant scales of the phenomenon can adequately be resolved by three-dimensional simulations. The main idea is to compare the performance of a swimmer where the swimming law is a backward traveling wave of given amplitude and frequency, to a swimming mode where the fin deformation mimics that of an elastic medium.

The modeling of the flow past a deformable body and the numerical methods are basically the same as those described in [5] and [2], *i.e.* we use cartesian grids where the body is modeled thanks to penalization and immersed boundary method. We considered a swimmer geometry similar to that a bluefin tuna [1]. The swimming law is obtained deforming as a function of time the midline in a plan $z = 0$. According to the literature, the midline is deformed in the plan $z = 0$ using the sinusoidal (swimming) law [1, 2] $y(x) = a(x)\sin(kx - \omega t)$, where $k = 2\pi/\lambda$ denotes the wave number associated with a wavelength λ and $\omega = 2\pi f$ denotes the pulsation of the oscillations associated with frequency f. We chose $a(x) = c_1 x$ where c_1 is fit to reach a desired maximal tail excursion, noted A.

The objective is to compare swim performance relative to different tail rigidities. To this end, the deformation can be imposed on a portion of the midline excluding the caudal fin. The caudal fin corresponds to the part of the midline between 0.8 and 1. In this region we model the fin by a lumped parameter elastic medium. The elastic caudal tail is composed by rigid struts joined by elastic links. Each link is subject to a couple C_i that is proportional to the square of the local tangential speed V_{i+1} of the next junction. To simplify the model, we assume that the inertia forces of the struts following the one considered are negligible, so that we have $\ddot{\theta}_i + \beta\dot{\theta}_i + k\theta_i = C_i, \quad i = 1, ..N_L - 1$ where θ_i is the rotation angle with respect to the previous strut, $C_i = -\alpha|V_{i+1}|V_{i+1}$, N_L is the number of links. The point $i = 0$ corresponds to 0.8 of the midline and is the last point where the deformation is explicitly imposed. The initial condition is $\theta_i = 0$, $\forall i$. Hence, for an infinitely rigid tail $\theta_i = 0$, $\forall i$. In the following examples we let $\beta = 1$, $k = 4 \cdot 10^3$, $0 \leq \alpha \leq 16 \cdot 10^{-2}$ and $N_L = 60$.

We compute the forces $\boldsymbol{F}$ and the torques $\boldsymbol{M}$ to compute the swimmer displacement. The velocity at the swimmer surface is $\boldsymbol{u}_s = \overline{\boldsymbol{u}} + \widehat{\boldsymbol{u}} + \widetilde{\boldsymbol{u}}$. where $\widetilde{\boldsymbol{u}}$ is the imposed deformation velocity, $\overline{\boldsymbol{u}}$ is the translation velocity and $\widehat{\boldsymbol{u}}$ is the rigid rotation velocity. The propulsive efficiency can be defined as [6]

$$\eta = \frac{W_{useful}}{W_{total}},$$

where W_{total} and W_{useful} are total and useful work of the swimmer over one stroke. The force exerted by the fluid on the body surface $\partial\Omega_s^i$ is $\boldsymbol{F}^i = (F_x^i, F_y^i, F_z^i)^T$. The total work of swimmer over one stroke T is then $W_{total} = \int_T \sum_{i=1}^{N_s} \boldsymbol{F}^i \cdot \boldsymbol{u}^i \, \mathrm{d}t$, where $\boldsymbol{u}^i$ is the average velocity on the surface $\partial\Omega_s^i$. The useful work is defined as the part of the total work corresponding to forces exerted in the swimming direction [6]. For instance, if the swimmer velocity is positive in the x-direction, $U_x > 0$, the useful force is $(F_x + |F_x|)/2$. The useful work is thus $W_{useful} = \int_T \sum_{i=1}^{N_s} \frac{F_x^i + |F_x^i|}{2} U_x^i \, \mathrm{d}t$.

All our results correspond to a Reynolds number $Re = \frac{U\ell}{\nu} = 10^3$. Such low Reynolds number is chosen so that we can consider that the flow is fully resolved. For instance, using $\nu = 10^{-6}$ for a fish swimming at a velocity around one body length per time unit, $Re = 10^3$ can be thought as relative for instance to a small fish of $3.16\,cm$ long Numerical experiments show that the rigidity parameter α should vary between 0.02 (rigid tail) and 0.16 (soft tail). The variation of the efficiency versus the rigidity parameter α for $f = 2$ are shown in figure 1(a). A value of $\alpha = 0.1$ maximize the efficiency. The flexible tail increases the efficiency of about 25% in comparison with the case where the deformation is applied onto the whole body.

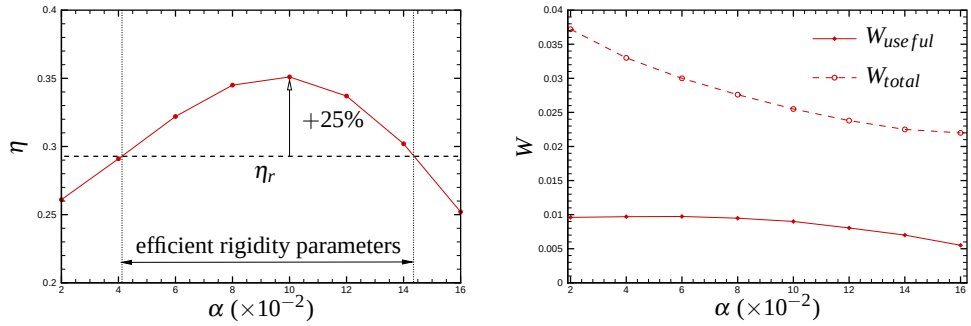

(a) η vs.α (b) W_{useful} and W_{total} vs. α

Figure 1: Evolution of the efficiency η, the useful work W_{useful} and the total work W_{total} versus the rigidity parameter α. Dotted line correspond to imposed tail deformation.

(a) $N_L = 1$ (b) $N_L = 3$ (c) $N_L = 60$

Figure 2: Swimmer shapes for different values of the number of links N_L. The case $N_L = 60$ correspond to $\alpha = 0.12$.

In what follows we investigate the influence of the curvature on the swimming efficiency. In the previous simulation we took $N_L = 60$ links on the tail. In what follows we take $1 \leq N_L \leq 5$ as presented in figure 2. The case $N_L = 60$ corresponds to $\alpha = 0.12$. The parameter α is modified for $1 \leq N_L \leq 5$ so that the phase tail portraits are as close as possible to the one for $N_L = 60$ with $\alpha = 0.12$. Note that the shape for $N_L = 5$ is similar to that with $N_L = 60$. Figure 3(a) shows that efficiency is enhanced when curvature is increased (N_L is increased). The evolution of the useful and total versus with the number of links N_L in presented in figure 3(b). While the value of the useful work is almost constant with N_L, the value of the total work done by the swimmer over one stroke decreases when N_L increases to reach the value obtained for our limit test case with $N_L = 60$.

The largest forces and velocities on the swimmer are located on the tail. In order to get a simple interpretation of the full simulations, we focus on the last tail segment, denoted by κ. Let $\boldsymbol{e}_\theta$ be the normal to κ as in figure 4. The relative velocity of the mid point of κ is noted $\boldsymbol{v} = (v_x, v_y)$ and let the force exerted by κ on the fluid be $\boldsymbol{F}$. The normal component of this force is mainly generated by the pressure jump, whereas the tangential force is generated by viscous effects. As a first approximation we neglect the viscous contributions ($Re \to \infty$). In this limit, we model the force by $\widetilde{\boldsymbol{F}} = (f_x, f_y) = \beta(\boldsymbol{e}_\theta \cdot \boldsymbol{v})|\boldsymbol{v}|\boldsymbol{e}_\theta$, $\beta > 0$. Thrust is generated when $f_x > 0$. The useful work model is then $\widetilde{W}_{useful} = \int_T \frac{f_x + |f_x|}{2} v_x \mathrm{d}t$. The work generated by lateral motion is $\int_T f_y v_y \mathrm{d}t$, and the total work is $\widetilde{W}_{total} = \int_T \widetilde{\boldsymbol{F}} \cdot \boldsymbol{v} \mathrm{d}t$. The efficiency resulting from this model is then $\widetilde{\eta} = \frac{\widetilde{W}_{useful}}{\widetilde{W}_{total}}$. Figure 5(b) shows the evolution of $\widetilde{W}_{useful}$ and $\widetilde{W}_{total}$ versus α. We scaled β ($\beta = 0.06$) so that the useful and total works are in the same ranges of figure 1(b). The tendencies are similar to those obtained in figure 5(b), except for the largest values of α. The plot of $\widetilde{\eta}$ versus α is presented in figure 5(a). Even if the values of $\widetilde{\eta}$ are slightly different from that of η obtained in figure 1(a), the tendency is similar. Indeed, the maximum efficiency is obtained for

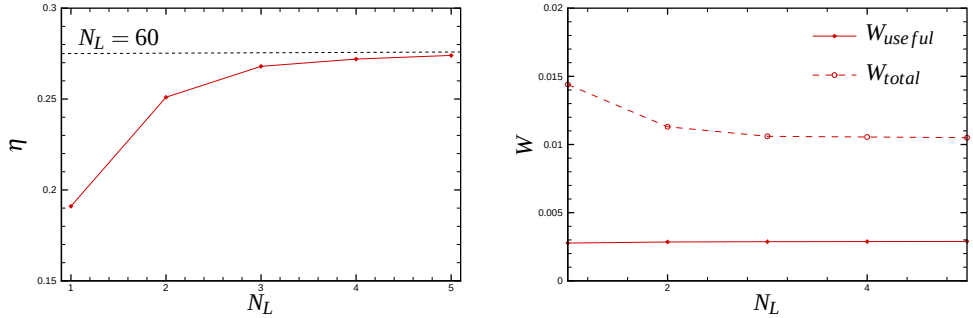

(a) η vs. N_L for $V = 0.4$ (b) W_{useful} and W_{total} vs. N_L for $V = 0.4$

Figure 3: Evolution of the efficiency η, the useful work W_{useful} and the total work W_{total} versus the number of links N_L for $V = 0.4$. Dotted line correspond to imposed tail deformation for $V = 0.4$

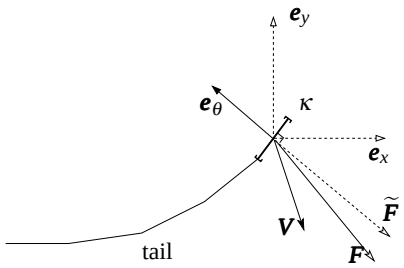

Figure 4: Sketch of the tail for the simplified efficiency approximation.

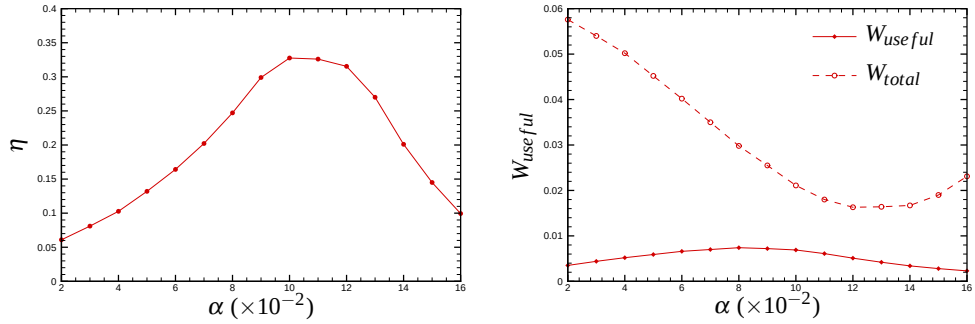

(a) η vs. α (b) W_{useful} and W_{total} vs. α

Figure 5: Evolution of the efficiency $\widetilde{\eta}$, the useful work $\widetilde{W}_{useful}$ and the total work $\widetilde{W}_{total}$ versus the rigidity parameter α. Dotted line correspond to imposed tail deformation.

the same parameter $\alpha = 0.12$ in both cases.

Our numerical results show that allowing a tail deformation induced by a simple elastic model has a marked influence on the swimmer propulsion. We show that a limited number of links (3) in the tail is able to warrant tail curvatures sufficient to reach efficiencies obtained with larger number of links. A simple model based on the kinematics of the last tail element can explain the efficiency improvement obtained and provide design indications on how to build an efficient tail for bio-mimetic swimming. These results may lead to significant improvements in the design of underwater robots.

REFERENCES

[1] D.S. Barrett, M.S. Triantafyllou, D.K.P. Yue, M.A. Grosenbauch, and M.J. Wolfgang. Drag reduction in fish-like locomotion. *J. Fluid Mech.*, 392:182–212, 1999.

[2] M. Bergmann and A. Iollo. Modeling and simulation of fish-like swimming. *Journal of Computational Physics*, 230(2):329 – 348, 2011.

[3] H. Dong, M. Bozkurttas, R. Mittal, P. Madden, and G.V. Lauder. Computational modeling and analysis of the hydrodynamics of a highly deformable fish pectoral fin. *Journal of Fluid Mechanics*, 645:345–373, 2010.

[4] C J Esposito, J L Tangorra, B E Flammang, and G V LAUDER. A robotic fish caudal fin: effects of stiffness and motor program on locomotor performance. *Journal of Experimental Biology*, 215(1):56–67, December 2011.

[5] R. Mittal, H. Dong, M. Bozkurttas, F.M. Najjar, A. Vargas, and A. von Loebbecke. A versatile sharp interface immersed boundary method for incompressible flows with complex boundaries. *Journal of Computational Physics*, 227(10):4825 – 4852, 2008.

[6] A. von Loebbecke, R. Mittal, F. Fish, and R. Mark. Propulsive efficiency of the underwater dolphin kick in humans. *J Biomech Eng.*, 131(5):054504, 2009.